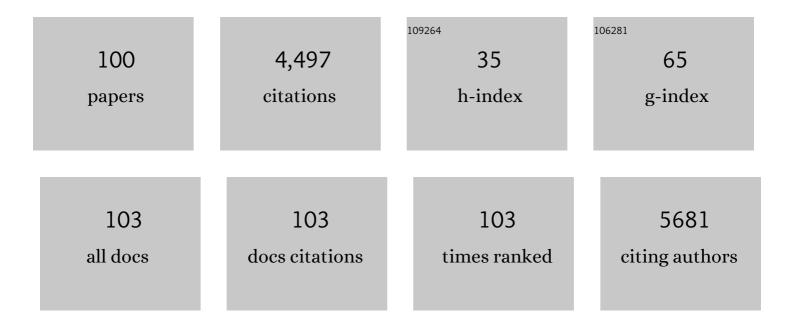
Jeong Min Baik

List of Publications by Year in descending order

Source: https://exaly.com/author-pdf/4029084/publications.pdf Version: 2024-02-01



#	Article	IF	CITATIONS
1	Hydrophobic Sponge Structureâ€Based Triboelectric Nanogenerator. Advanced Materials, 2014, 26, 5037-5042.	11.1	426
2	Boosted output performance of triboelectric nanogenerator via electric double layer effect. Nature Communications, 2016, 7, 12985.	5.8	336
3	Mesoporous pores impregnated with Au nanoparticles as effective dielectrics for enhancing triboelectric nanogenerator performance in harsh environments. Energy and Environmental Science, 2015, 8, 3006-3012.	15.6	315
4	Highly Stretchable 2D Fabrics for Wearable Triboelectric Nanogenerator under Harsh Environments. ACS Nano, 2015, 9, 6394-6400.	7.3	310
5	Robust nanogenerators based on graft copolymers via control of dielectrics for remarkable output power enhancement. Science Advances, 2017, 3, e1602902.	4.7	204
6	Embossed Hollow Hemisphereâ€Based Piezoelectric Nanogenerator and Highly Responsive Pressure Sensor. Advanced Functional Materials, 2014, 24, 2038-2043.	7.8	124
7	Pd-Sensitized Single Vanadium Oxide Nanowires: Highly Responsive Hydrogen Sensing Based on the Metalâ^'Insulator Transition. Nano Letters, 2009, 9, 3980-3984.	4.5	121
8	Highly anisotropic power generation in piezoelectric hemispheres composed stretchable composite film for self-powered motion sensor. Nano Energy, 2015, 11, 1-10.	8.2	121
9	High humidity- and contamination-resistant triboelectric nanogenerator with superhydrophobic interface. Nano Energy, 2019, 57, 903-910.	8.2	119
10	Tin-Oxide-Nanowire-Based Electronic Nose Using Heterogeneous Catalysis as a Functionalization Strategy. ACS Nano, 2010, 4, 3117-3122.	7.3	99
11	Silk fibroin-based biodegradable piezoelectric composite nanogenerators using lead-free ferroelectric nanoparticles. Nano Energy, 2015, 14, 87-94.	8.2	97
12	Polarized Surface-Enhanced Raman Spectroscopy from Molecules Adsorbed in Nano-Gaps Produced by Electromigration in Silver Nanowires. Nano Letters, 2009, 9, 672-676.	4.5	84
13	Electrospun ion gel nanofibers for flexible triboelectric nanogenerator: electrochemical effect on output power. Nanoscale, 2015, 7, 16189-16194.	2.8	79
14	Selfâ€Powered, Roomâ€Temperature Electronic Nose Based on Triboelectrification and Heterogeneous Catalytic Reaction. Advanced Functional Materials, 2015, 25, 7049-7055.	7.8	76
15	Highâ€Output Triboelectric Nanogenerator Based on Dual Inductive and Resonance Effectsâ€Controlled Highly Transparent Polyimide for Selfâ€Powered Sensor Network Systems. Advanced Energy Materials, 2019, 9, 1901987.	10.2	73
16	Growth of Metal Oxide Nanowires from Supercooled Liquid Nanodroplets. Nano Letters, 2009, 9, 4138-4146.	4.5	70
17	Effect of microstructural change on magnetic property of Mn-implanted p-type GaN. Applied Physics Letters, 2003, 82, 583-585.	1.5	69
18	The Progress of PVDF as a Functional Material for Triboelectric Nanogenerators and Self-Powered Sensors. Micromachines, 2018, 9, 532.	1.4	64

#	Article	IF	CITATIONS
19	Transparent-flexible-multimodal triboelectric nanogenerators for mechanical energy harvesting and self-powered sensor applications. Nano Energy, 2018, 48, 471-480.	8.2	63
20	Self-Assembled and Highly Selective Sensors Based on Air-Bridge-Structured Nanowire Junction Arrays. ACS Applied Materials & amp; Interfaces, 2013, 5, 6802-6807.	4.0	62
21	Nanostructure-Dependent Metalâ^'Insulator Transitions in Vanadium-Oxide Nanowires. Journal of Physical Chemistry C, 2008, 112, 13328-13331.	1.5	58
22	Surface dipole enhanced instantaneous charge pair generation in triboelectric nanogenerator. Nano Energy, 2016, 26, 360-370.	8.2	54
23	Sustainable highly charged C ₆₀ -functionalized polyimide in a non-contact mode triboelectric nanogenerator. Energy and Environmental Science, 2021, 14, 1004-1015.	15.6	52
24	Research Update: Recent progress in the development of effective dielectrics for high-output triboelectric nanogenerator. APL Materials, 2017, 5, .	2.2	51
25	Highly efficient organic light-emitting diodes with hole injection layer of transition metal oxides. Journal of Applied Physics, 2005, 98, 093707.	1.1	49
26	High-yield TiO2 nanowire synthesis and single nanowire field-effect transistor fabrication. Applied Physics Letters, 2008, 92, .	1.5	47
27	Fe Nanowires in Nanoporous Alumina:  Geometric Effect versus Influence of Pore Walls. Journal of Physical Chemistry C, 2008, 112, 2252-2255.	1.5	46
28	Enhancing Light Emission of Nanostructured Vertical Lightâ€Emitting Diodes by Minimizing Total Internal Reflection. Advanced Functional Materials, 2012, 22, 632-639.	7.8	46
29	All-Transparent NO ₂ Gas Sensors Based on Freestanding Al-Doped ZnO Nanofibers. ACS Applied Electronic Materials, 2019, 1, 1261-1268.	2.0	45
30	Facile Synthesis of Single Crystalline Metallic RuO ₂ Nanowires and Electromigration-Induced Transport Properties. Journal of Physical Chemistry C, 2011, 115, 4611-4615.	1.5	42
31	Design of Mechanical Frequency Regulator for Predictable Uniform Power from Triboelectric Nanogenerators. Advanced Energy Materials, 2018, 8, 1702667.	10.2	42
32	3D printed noise-cancelling triboelectric nanogenerator. Nano Energy, 2017, 38, 377-384.	8.2	41
33	Electrothermally Induced Highly Responsive and Highly Selective Vanadium Oxide Hydrogen Sensor Based on Metal–Insulator Transition. Journal of Physical Chemistry C, 2012, 116, 226-230.	1.5	40
34	Zero-dimensional heterostructures: N-doped graphene dots/SnO ₂ for ultrasensitive and selective NO ₂ gas sensing at low temperatures. Journal of Materials Chemistry A, 2020, 8, 11734-11742.	5.2	39
35	A built-in electric field induced by ferroelectrics increases halogen-free organic solar cell efficiency in various device types. Nano Energy, 2020, 68, 104327.	8.2	38
36	Self-powered triboelectric aptasensor for label-free highly specific thrombin detection. Nano Energy, 2016, 30, 77-83.	8.2	35

#	Article	IF	CITATIONS
37	Enhanced piezoresponse of highly aligned electrospun poly(vinylidene fluoride) nanofibers. Nanotechnology, 2017, 28, 395402.	1.3	34
38	Plasmonic gold nanoparticle-decorated BiVO ₄ /ZnO nanowire heterostructure photoanodes for efficient water oxidation. Catalysis Science and Technology, 2018, 8, 3759-3766.	2.1	34
39	3D Cu ball-based hybrid triboelectric nanogenerator with non-fullerene organic photovoltaic cells for self-powering indoor electronics. Nano Energy, 2020, 77, 105271.	8.2	33
40	A composite of a graphene oxide derivative as a novel sensing layer in an organic field-effect transistor. Journal of Materials Chemistry C, 2014, 2, 4539-4544.	2.7	32
41	Highly Branched RuO ₂ Nanoneedles on Electrospun TiO ₂ Nanofibers as an Efficient Electrocatalytic Platform. ACS Applied Materials & Interfaces, 2015, 7, 15321-15330.	4.0	32
42	Enhancement of magnetic properties by nitrogen implantation to Mn-implanted p-type GaN. Applied Physics Letters, 2004, 84, 1120-1122.	1.5	31
43	Electronic Structure and Magnetism in Transition Metals Doped 8-Hydroxy-Quinoline Aluminum. Journal of the American Chemical Society, 2008, 130, 13522-13523.	6.6	31
44	Highly-sensitive and highly-correlative flexible motion sensors based on asymmetric piezotronic effect. Nano Energy, 2018, 51, 185-191.	8.2	29
45	Remarkable output power enhancement of sliding-mode triboelectric nanogenerator through direct metal-to-metal contact with the ground. Nano Energy, 2019, 57, 293-299.	8.2	28
46	ZnO Nanowire-Based Antireflective Coatings with Double-Nanotextured Surfaces. ACS Applied Materials & Interfaces, 2014, 6, 1375-1379.	4.0	24
47	Ferroelectrically augmented contact electrification enables efficient acoustic energy transfer through liquid and solid media. Energy and Environmental Science, 2022, 15, 1243-1255.	15.6	24
48	The effects of implanted nitrogen ions on the magnetic properties of Mn-implanted GaN. Metals and Materials International, 2004, 10, 555-558.	1.8	22
49	Strategies for ultrahigh outputs generation in triboelectric energy harvesting technologies: from fundamentals to devices. Science and Technology of Advanced Materials, 2019, 20, 927-936.	2.8	22
50	Two-dimensional metal-dielectric hybrid-structured film with titanium oxide for enhanced visible light absorption and photo-catalytic application. Nano Energy, 2016, 21, 115-122.	8.2	21
51	Boosting the energy conversion efficiency of a combined triboelectric nanogenerator-capacitor. Nano Energy, 2019, 56, 571-580.	8.2	20
52	Effect of microstructural evolution on magnetic property of Mn-implanted p-type GaN. Applied Physics Letters, 2003, 83, 2632-2634.	1.5	19
53	Structural Evolution of Chemically-Driven RuO2 Nanowires and 3-Dimensional Design for Photo-Catalytic Applications. Scientific Reports, 2015, 5, 11933.	1.6	19
54	Gate-Tunable Spin Exchange Interactions and Inversion of Magnetoresistance in Single Ferromagnetic ZnO Nanowires. ACS Nano, 2016, 10, 4618-4626.	7.3	19

#	Article	lF	CITATIONS
55	Parallel Aligned Mesopore Arrays in Pyramidal-Shaped Gallium Nitride and Their Photocatalytic Applications. ACS Applied Materials & Interfaces, 2016, 8, 18201-18207.	4.0	18
56	Triboelectric Charge-Driven Enhancement of the Output Voltage of BiSbTe-Based Thermoelectric Generators. ACS Energy Letters, 2021, 6, 1095-1103.	8.8	18
57	Automatically switchable mechanical frequency regulator for continuous mechanical energy harvesting via a triboelectric nanogenerator. Nano Energy, 2021, 89, 106350.	8.2	17
58	Rhodium-oxide-coated indium tin oxide for enhancement of hole injection in organic light emitting diodes. Applied Physics Letters, 2005, 87, 072105.	1.5	16
59	Mechanically Robust, Stretchable Solar Absorbers with Submicron-Thick Multilayer Sheets for Wearable and Energy Applications. ACS Applied Materials & Interfaces, 2017, 9, 18061-18068.	4.0	16
60	Unidirectional growth of single crystalline l²-Na _{0.33} V ₂ O ₅ and l̂±-V ₂ O ₅ nanowires driven by controlling the pH of aqueous solution and their electrochemical performances for Na-ion batteries. CrystEngComm, 2017, 19, 5028-5037.	1.3	16
61	A thermodynamic approach toward selective and reversible sub-ppm H ₂ S sensing using ultra-small CuO nanorods impregnated with Nb ₂ O ₅ nanoparticles. Journal of Materials Chemistry A, 2021, 9, 17425-17433.	5.2	16
62	Phase-Tuned MoS ₂ and Its Hybridization with Perovskite Oxide as Bifunctional Catalyst: A Rationale for Highly Stable and Efficient Water Splitting. ACS Applied Materials & Interfaces, 2022, 14, 18248-18260.	4.0	16
63	Fabrication of (Ga,Mn)N nanowires with room temperature ferromagnetism using nitrogen plasma. Applied Physics Letters, 2005, 87, 042105.	1.5	14
64	Directional Ostwald Ripening for Producing Aligned Arrays of Nanowires. Nano Letters, 2019, 19, 4306-4313.	4.5	14
65	Wide-temperature (up to 100°C) operation of thermostable vanadium oxide based microbolometers with Ti/MgF2 infrared absorbing layer for long wavelength infrared (LWIR) detection. Applied Surface Science, 2021, 547, 149142.	3.1	14
66	Threeâ€Dimensional Branched Nanowire Heterostructures as Efficient Lightâ€Extraction Layer in Lightâ€Emitting Diodes. Advanced Functional Materials, 2014, 24, 3384-3391.	7.8	13
67	Photo-stimulated triboelectric generation. Nanoscale, 2017, 9, 18597-18603.	2.8	13
68	Alternatively driven dual nanowire arrays by ZnO and CuO for selective sensing of gases. Sensors and Actuators B: Chemical, 2013, 185, 10-16.	4.0	12
69	Enhanced performance of a direct contact membrane distillation (DCMD) system with a Ti/MgF2 solar absorber under actual weather environments. Desalination, 2020, 491, 114580.	4.0	11
70	Ce oxide nanoparticles on porous reduced graphene oxides for stable hydrogen detection in air/HMDSO environment. Sensors and Actuators B: Chemical, 2020, 321, 128529.	4.0	11
71	Graphene-Assisted Zwitterionic Conjugated Polycyclic Molecular Interfacial Layer Enables Highly Efficient and Stable Inverted Perovskite Solar Cells. Chemistry of Materials, 2021, 33, 5563-5571.	3.2	11
72	Enhancement of magnetic properties in (Ga,Mn)N nanowires due to N2 plasma treatment. Applied Physics Letters, 2006, 89, 152113.	1.5	10

#	Article	IF	CITATIONS
73	Correlation between thermal annealing temperature and Joule-heating based insulator-metal transition in VO2 nanobeams. Applied Physics Letters, 2013, 103, 203114.	1.5	9
74	A Wide Dynamic Range Multi-Sensor ROIC for Portable Environmental Monitoring Systems With Two-Step Self-Optimization Schemes. IEEE Transactions on Circuits and Systems I: Regular Papers, 2021, 68, 2432-2443.	3.5	9
75	Visible Color Tunable Emission in Three-Dimensional Light Emitting Diodes by MgO Passivation of Pyramid Tip. ACS Applied Materials & Interfaces, 2015, 7, 27743-27748.	4.0	8
76	A large-area fabrication of moth-eye patterned Au/TiO2 gap-plasmon structure and its application to plasmonic solar water splitting. Solar Energy Materials and Solar Cells, 2019, 201, 110033.	3.0	8
77	Output signals control of triboelectric nanogenerator with metal-dielectric-metal configuration through high resistance grounded systems. Nano Energy, 2022, 95, 107023.	8.2	8
78	Lowâ€Temperature Deâ€NO <i>_x</i> Extruded Monolithic Catalysts Based on Highly Dispersive Mn–Ce Oxide Nanoparticles of Low Ce Content. Advanced Materials Technologies, 2019, 4, 1800462.	3.0	7
79	Solutionâ€Processed Graphene Thinâ€Film Enables Binderâ€Free, Efficient Loading of Nanocatalysts for Electrochemical Water Splitting. Advanced Materials Interfaces, 2021, 8, 2101576.	1.9	7
80	Ferromagnetic properties of (Ga,Mn)N nanowires grown by a chemical vapor deposition method. Journal of Vacuum Science & Technology an Official Journal of the American Vacuum Society B, Microelectronics Processing and Phenomena, 2005, 23, 530.	1.6	6
81	Optical design of ZnO-based antireflective layers for enhanced GaAs solar cell performance. Physical Chemistry Chemical Physics, 2016, 18, 2906-2912.	1.3	6
82	Pyramidal Metal–dielectric hybrid-structure geometry with an asymmetric TiO2 layer for broadband light absorption and photocatalytic applications. Nano Energy, 2018, 53, 468-474.	8.2	5
83	Photo-stimulated charge transfer in contact electrification coupled with plasmonic excitations. Nano Energy, 2019, 65, 104031.	8.2	5
84	Triple layered Ga ₂ O ₃ /Cu ₂ O/Au photoanodes with enhanced photoactivity and stability prepared using iron nickel oxide catalysts. Journal of Materials Chemistry A, 2020, 8, 10966-10972.	5.2	5
85	Development of a Novel Gas-Sensing Platform Based on a Network of Metal Oxide Nanowire Junctions Formed on a Suspended Carbon Nanomesh Backbone. Sensors, 2021, 21, 4525.	2.1	5
86	3D Multiscale Gradient Pores Impregnated with Ag Nanowires for Simultaneous Pressure and Bending Detection with Enhanced Linear Sensitivity. Advanced Materials Technologies, 2020, 5, 1901041.	3.0	5
87	Observation of ferromagnetic ordering in Mnâ€doped 8â€hydroxyâ€quinoline aluminum. Physica Status Solidi - Rapid Research Letters, 2008, 2, 22-24.	1.2	4
88	Modulating ZnO Nanostructure Arrays on Any Substrates by Nanolevel Structure Control. Journal of Physical Chemistry C, 2011, 115, 7987-7992.	1.5	4
89	High rotational speed hand-powered triboelectric nanogenerator toward a battery-free point-of-care detection system. RSC Advances, 2021, 11, 23221-23227.	1.7	4
90	Unprecedented Insulator-to-Metal Transition Dynamics by Heterogeneous Catalysis in Pd-Sensitized Single Vanadium Oxide Nanowires. Journal of Physical Chemistry C, 2013, 117, 21864-21869.	1.5	3

#	Article	IF	CITATIONS
91	Circuit Modeling Approach for Analyzing Triboelectric Nanogenerators for Energy Harvesting. , 2018, , .		3
92	The migration of alkali metal (Na+, Li+, and K+) ions in single crystalline vanadate nanowires: Rasch-Hinrichsen resistivity. Current Applied Physics, 2019, 19, 516-520.	1.1	3
93	Co-implantation of Mn+ N into p-type GaN for highTC ferromagnetism. Physica Status Solidi C: Current Topics in Solid State Physics, 2003, 0, 2878-2881.	0.8	2
94	Energy Harvesting: Design of Mechanical Frequency Regulator for Predictable Uniform Power from Triboelectric Nanogenerators (Adv. Energy Mater. 15/2018). Advanced Energy Materials, 2018, 8, 1870072.	10.2	2
95	Graphene Antiadhesion Layer for the Effective Peel-and-Pick Transfer of Metallic Electrodes toward Flexible Electronics. ACS Applied Materials & Interfaces, 2021, 13, 22000-22008.	4.0	2
96	3D Multiple Triangular Prisms for Highly Sensitive Non-Contact Mode Triboelectric Bending Sensors. Nanomaterials, 2022, 12, 1499.	1.9	2
97	Electrocatalytically driven fast removal of moisture by condensation of vapor and water splitting. Nano Energy, 2019, 61, 295-303.	8.2	1
98	Realistic Circuit Modeling Using Derating Factors for Triboelectric Nanogenerators in Energy Harvesting Applications. , 2019, , .		1
99	Electric-Field Induced Abrupt and Multi-Step Insulator-Metal Transitions in Vanadium Dioxide Nanobeams. Journal of Nanoscience and Nanotechnology, 2017, 17, 4247-4250.	0.9	0
100	Solutionâ€Processed Graphene Thinâ€Film Enables Binderâ€Free, Efficient Loading of Nanocatalysts for Electrochemical Water Splitting (Adv. Mater. Interfaces 23/2021). Advanced Materials Interfaces, 2021, 8, .	1.9	0